Published in final edited form as:
J Comput Chem. 2011 April 15; 32(5): 854–865. doi:10.1002/jcc.21663.

The Opsin Shift and Mechanism of Spectral Tuning of Rhodopsin

Ramkumar Rajamani[a], **Yen-Ilin Lin**, and **Jiali Gao**
Department of Chemistry, Digital Technology Center, and Supercomputing Institute, University of Minnesota, Minneapolis, MN 55455

Jiali Gao: gao@jialigao.org

Abstract

Molecular dynamics simulations and combined quantum mechanical and molecular mechanical (QM/MM) calculations have been performed to investigate the mechanism of the opsin shift and spectral tuning in rhodopsin. A red shift of −980 cm^{-1} was estimated in the transfer of the chromophore from methanol solution environment to the protonated Schiff base binding site of the opsin. The conformational change from a 6-s-cis-all-trans configuration in solution to the 6-s-cis-11-cis conformer contributes additional −200 cm^{-1} and the remaining effects were attributed to dispersion interactions with the aromatic residues in the binding site. An opsin shift of 2100 cm^{-1} was obtained, in reasonable accord with experiment (2730 cm^{-1}). Dynamics simulations revealed that the 6-s-cis bond can occupy two main conformations for the β-ionone ring, resulting a weighted average dihedral angle of about 50°, which may be compared with the experimental estimate of −28° from solid-state NMR and Raman data. We investigated a series of four single-mutations, including E113D, A292S, T118A and A269T, which are located near the protonated Schiff base, along the polyene chain of retinal and close to the ionone ring. The computational results on absorption energy shift provided insights into the mechanism of spectral tuning, which involves all means of electronic structural effects, including the stabilization or destabilization of either the ground or the electronically excited state of the retinal protonated Schiff base.

Introduction

The ability for the human eye to distinguish a variety of shades of colors is determined by the chromophore 11-*cis* retinal, which is covalently bound to Lys296 of rhodopsin through a protonated Schiff base (PSB) linkage.[1,2] Human visual pigments are found in the rod and cone cells that line the outer layer of retina. The pigment in the rod cells mediates scotopic (dark) vision with a maximum absorption wavelength (λ_{max}) of 500 nm. The cone cells contain three pigments responsible for color vision, with maximum absorption wavelength corresponding to regions in blue (λ_{max} = 425 nm), green (λ_{max} = 533 nm), and red (λ_{max} = 560nm).[1–4] These pigments consist of a chromophore retinal (11-s-cis), and a protein called "opsin", which is a single polypeptide, containing seven transmembrane α-helices, a feature common to G-protein coupled receptors (GPCR).[5,6] The opsin shift refers to the difference between the observed λ_{max} of the retinal PSB in methanol solution[7] and that in the opsin.[3,4,8] We aim to provide an understanding of the origin of the absorption energy shifts (spectral tuning) in rhodopsin, making use of combined quantum mechanical and molecular mechanical (QM/MM) methods and molecular dynamics simulations.

Correspondence to: Jiali Gao, gao@jialigao.org.

[a]Present address: Department of Computer-Assisted Drug Design, Bristol-Myers Squibb Pharmaceutical Research Institute, 5 Research Parkway, Wallingford, CT 06492. ramkumar.rajamani@bms.com

There have been numerous experimental and theoretical studies of spectral regulation of the PSB in rhodopsins.[8–43] Broadly, four factors have been identified to contribute to the observed spectral shifts;[18,19,44,45] they include counterion effects (or a change of electrostatic interactions of the chromophore with the solvent and with the protein), specific charge interactions (partial charges interacting with the polyene chain), dispersion interactions due to aromatic sidechains surrounding the chromophore and structural changes in the chromophore conformation. The main new finding of the present study is the mechanism of spectral tuning which involves a combination of factors, including the stabilization or destabilization of either the ground state or the excited electronic state through individual amino acid mutations.

In the absence of structural information, Honig and coworkers proposed an external point charge model to explain the opsin shift in bovine rhodopsin,[7,17,18,46–48] while site-directed mutations established that Asp113 is the primary counterion of the protonated schiff base (PSB).[49–51] The early biochemical findings have been confirmed by crystal structures,[52] which revealed that the sidechain oxygen atoms of Asp113 are 3.3 and 3.5 Å from the Schiff base nitrogen in bovine rhodopsin. Other residues in the PSB-binding site also play important roles in modulating the absorption spectra through electrostatic and dispersion interactions. In general, dispersion interactions stabilize the π^* excited state more strongly than they stabilize the ground state,[44] and the significance of such effects in the rhodopsin spectral tuning is evident by the presence of a number of aromatic residues along the retinal polyene chain. Previous studies on bacteriorhodopsin by Yan et. al. have shown that the combined contribution of the polar residues, β-ionone ring and dispersion polarization results in a red shift of 2000 cm^{-1},[53] and Houjou et al. estimated that the dispersion contribution to the opsin shift is about 1000 cm^{-1}.[19]

The contribution due to conformational changes of PSB, arises from the effect on delocalization of charge density along the polyene chain.[54] Charge delocalization in the excited state depends on the twisting of the polyene chain about the single and double bonds. Twisting along single bonds causes a decrease in the π delocalization, leading to a net blue shift in the absorption maxima,[24,55] whereas an increase in delocalization over an extended double bond system can result in red shift in the absorption maxima.[24,56] Thus the change in a preferred conformation of the PSB in solutions and in the gas phase to that within the enzyme environment contributes to the total opsin shift.

One of the most remarkable properties of rhodopsin is its ability to adjust the maximum absorption wavelength in the three pigments to encompass the entire range of visible light. Bovine Rhodopsin is among the most widely studied because of its importance to mammalian vision and ease in preparation.[57,58] The human visual pigments, though optimized by nature to absorb at characteristic wavelengths, have a high degree of sequence homology. The green and red pigments have 96% sequence homology, differing only at 15 positions, but the maximum absorption wavelengths differ by 30 nm, or about 1000 cm^{-1} in energy. The difference between the blue and red pigments is as large as more than 5500 cm^{-1}.[59] The high degree of similarity shows the significance of the strategic positioning of specific amino acids on the spectral character. For example, the replacement of seven of the fifteen residues account for the entire change in λ_{max} from ~530 nm (green) to ~560 nm (red), with three specific replacements making most of the contributions.[58] Mutations of the equivalent residues in bovine rhodopsin resulted in a red shift of 20 nm.[60] Other studies include simultaneous mutation of the nine residues that were identified through alignment of bovine rhodopsin and mammalian (human, rat, mouse, bovine) blue cone pigments; this multiple-mutation accounts for 80% of the observed spectral shift between the blue cone pigment and bovine rhodopsin.[61] Moreover, a host of single mutation studies have been

performed to understand the role of specific residues in spectral tuning in the visual pigments.[58,60,62–67]

On the theoretical side, there are two relevant questions. The first is the ability to accurately predict the absolute values of the absorption energies of different visual pigments. This is very important and is a difficult task because it is necessary to use high-level theoretical methods such as CASPT2 or time-dependent density functional theory (TD-DFT) with large basis sets.[23–25,28–42] Consequently, these applications are typically carried out using minimized chromophore geometries in a single protein configuration. It has been found that the computed vertical excitation energies are strongly dependent on the basis set used and the level of theory applied and the absorption spectra can vary as large as more than 200 nm. [24] Although useful insights can be obtained on the chromophore electronic structure, dynamic fluctuations of the protein environment are neglected, which provide key information on spectral line shape.[22,43] The second issue, which is the emphasis of the present study, is concerned with the change of the absorption energy maximum due to the change of the chromophore environment and amino acid mutations.[22,24,26,27,43,68–71] An understanding of the spectral shifts can help to elucidate the mechanism of spectral tuning in visual pigments.[22,24,43] The dominant contributing factors in the solvachromic shift are due to electrostatic interactions[20–22,72] and this can be adequately modeled by computationally less demanding methods including configuration interaction with only single excitations (CIS)[73,74] embedded in molecular mechanics force fields (CIS-QM/MM).[22,43,68–71,74] This approach has been applied to a variety of systems that show large solvatochromic shifts in solution,[68–70,74] and used to analyze various factors contributing to the observed opsin shift in bacteriorhodopsin,[22] and rhodopsin.[43]

Combined QM/MM calculations have been used in several studies of rhodopsin.[20,25–27,43,72], To understand the spectral shifts between bacteriorhodopsin (bR) and sensory rhodopsin II (SRII), Birge and coworkers used a combination of modified neglect of differential overlap and double configuration interaction (MNDO-PSDCI) techniques and identified that the difference in position of Arg-72 in SR(II) (Arg-82 in bR) was the major source of observed blue shift between the two proteins.[20] On the other hand, Schulten and co-workers, who employed a QM/MM-CASSCF (complete active space self-consistent field) model, concluded that electronic reorganization in the retinal Schiff base makes the dominant contribution to the bR to SRII spectral shift.[72] Subsequently, Hoffmann et al. carried out comprehensive investigations using semiempirical and ab initio multireference CI approaches, and found that neutral amino acids in the PSB binding pocket and the hydrogen bonding network on the extracellular side contribute about 90% of the total shift. [25–27] Trabanino et al. performed QM-CIS/MM calculations on three pigment structures generated by homology modeling and found that structural twisting and dipolar side chains in the PSB binding pocket contribute to the various spectral shifts.[43] The latter studies demonstrate that combined CIS-QM/MM studies can be used to understand specific protein-chromophore interactions.

The focus of this study is to elucidate the fundamental mechanism underlying the spectral tuning of visual pigments, using combined QM-CIS/MM methods and molecular dynamics simulations.[22,68] Our aim is not to reproduce the full absorption spectra of the three color pigments; rather, we wish to identify the origin of specific amino acid-chromophore interactions that alter the energies of the ground and excited electronic states of the chromophore, leading to the observed spectral shifts. Thus, we choose to use bovine rhodopsin and single amino-acid mutations in our investigation; bovine rhodopsin shares 88% sequence identity with human rhodopsin and has an identical maximum absorption wavelength at 500 nm, approximately in the mid-range of the visible spectrum. We have identified four residue mutations to illustrate the mechanism affecting the absorption energy;

they are Glu113 to Asp (E113D), Thr118 to Ala (T118A), Ala292 to Ser (A292S) and Ala269 to Thr (A269T). The selection was based on the location of these residues in the binding pocket, ranging from the PSB counterion site to the steric interactions at the ionone ring of the chromophore along with consideration of mutations in the blue and red visual cone pigments.

In the following, we first describe the computational details, followed by results and discussion. The paper concludes with a summary of major findings of the present study.

Computational Details

To investigate the origin of the opsin shift and the mechanism of spectral tuning in rhodopsin, we utilize a combination of techniques based on quantum mechanics and molecular mechanics. In a previous study, we have successfully applied a combined QM/MM approach to analyze the opsin shift in bacteriorhodopsin.[22] The same approach is employed in the present work. Here, we briefly summarize the computational procedure, focusing primarily on the simulation model relevant to rhodopsin.

A. Protein-Bilayer Modeling—We used the bovine rhodopsin structure (PDB code: 1HZX) to set up the initial protein-membrane-solvent system for molecular dynamics simulations.[75] A number of titratable residues, including E113, E122, E181 and H211, are located close to the binding site of the retinal chromophore. In the present study, all acidic residues (Glu and Asp) are negatively charged and histidine residues are kept neutral. There are eight amino acids that are disordered in the crystal structure; they are residues 236–240 and 331–333, which belong to the cytoplasmic loop II and the C-terminal. We have built the missing coordinates using the biopolymer module in the program InsightII. Initially, the two amino acid residues prior and two residues after the missing residues are defined as the anchor residues for the loop construction. Then, the sequence of the missing loop was compared with a database of loops derived from the protein databank, and the ten structures from the database that best fit the rhodopsin loop-sequence were selected. The inclusion of the missing residues positions was completed through the use of the splice facility within the module biopolymers of InsightII, which incorporates the coordinates of the previously selected loop into the target structure. The loop residues were energy-minimized for 200 steps using the adopted basis Newton-Raphson (ABNR)[76] method with the rest of the protein atomic positions held fixed. This yields a compete set of rhodopsin coordinates.

NMR and Fourier transform IR studies suggested the involvement of a water-mediated network between the Schiff base and its counterion E113.[77–79] However the crystal structure showed that the side chain of the counter ion is in direct contact with the PSB.[75] A total of 12 water positions were resolved in the crystal structure, one of which is about 4.4 Å away from the carboxylate group of E113. Through accessible surface calculations, the authors of the crystal structure reported the existence of two cavities located near the nitrogen of the Schiff base.[75] To probe the possibility of other possible positions for water, we used the program DOWSER to analyze the solvent cavity in the protein.[80] A probe radius of 1.4 Å was used and six cavities were identified to be large enough to accommodate water molecules. Along with the crystal water, a total of 18 waters were included in the initial coordinate set. The positions of the additional water molecules were optimized for 100 steps using the ABNR algorithm with the protein and crystal water positions held fixed.

The initial configuration of the membrane-protein complex was constructed using a procedure similar to that described by Wolf et al.[81] The protein was first placed in a orthorhombic box having a target dimension of roughly X = 159 Å, Y= 189 Å, and Z=200 Å, with its center of mass position coincide with the origin of the box. Then, the protein was oriented by aligning the principal axis of helix VI in the direction of the z-axis. This

reference was chosen based on the helical tilt analysis of the crystal structure presented by Teller, et al.,[75] suggesting that helix VI has an tilt angle of nearly zero with respect to the norm of the membrane surface and that the protein has dimensions of 41, 45 and 37Å in height and widths, respectively.[75] Based on the experimental surface area (64 $Å^2$)[82] for each lipid headgroup and the system dimension, a total of 70 DMPC (1,2-dimiristoyl-SN-glycero-3-phosphorylcholine) lipid molecules, half on each side, was used to embed the opsin molecule.

The positions of the lipids were constructed by the following procedure. First, 35 van der Waals spheres of radius 9 Å, mimicking the size of the lipid headgroup, were placed on each of the two x-y planes located at z = +17 Å and −17 Å, roughly the interfacial region between the bilayer and bulk water. The size of the planes was initially set to have three times of the target area. Then, 100 steps of energy minimization were performed, followed by 1 ps of molecular dynamics simulation at 300K, with the protein and water atoms held fixed. The van der Waals spheres were restrained to move only in the x-y plane. At the end of the molecular dynamics simulation, the sizes of the x-y plane for the van der Waals spheres were reduced by 1 Å in each direction, and this process was repeated until the final size of the x-y plane reached the target value. The resulting positions of the van der Waals spheres were used to anchor the lipid head groups by placing a randomly selected lipid molecular from a library of lipids configurations generated from molecular simulations.[83] Each lipid orientation was further optimized through rigid body rotation and translation to minimize close contacts. Finally, the system was solvated by overlaying two pre-equilibrated water boxes over the two planes of the bilayer head groups and water molecules that are within 2.6 Å of any protein or crystal water atoms were removed. The final dimension of the completed membrane-protein complex is X = 53 Å, Y = 63 Å, and Z = 93 Å, and the system contains 348 amino acid residues, 70 DMPC lipid molecules, 5979 Water molecules, and 3 Na^+ ions to neutralize the total charge of the system, giving rise to a total of 31763 atoms.

B. Simulation—All simulations were carried out using the CHARMM[76] program (c28a1) and the CHARMM22 force field.[84–86] The empirical parameters developed by Schulten and coworkers were used to describe the chromophore retinal,[87,88] and the three-point charge TIP3P model was used to represent water.[89] The isothermal-isobaric (NPT) ensemble at 330 K and 1 atm was used along with periodic boundary conditions. The Nose-Hoover thermostat was used to maintain the temperature and the pressure was controlled by the Anderson method and the Verlet algorithm[90] with an integration time step of 2 fs was used. All bonds and angles involving hydrogen atoms were constrained using SHAKE.[91] Structures were saved every 50 integration steps along the molecular trajectory. Long-range electrostatic interactions were included by using the particle mesh Ewald (PME) method, with the parameters of $\kappa = 0.32$ Å, order = 6, fftx = 64, ffty =64, and fftz =128.[92] After construction of the system, it was equilibrated for 1 ns, which was followed by additional 2 ns for analysis. A snap shot of the rhodopsin-membrane structure during the molecular dynamics simulation is shown in Figure 1. All calculations were performed on a cluster of IBM-SP computers at the Minnesota Supercomputing Institute (MSI) using 16 processors.

C. Spectral Analysis—The computed electronic excitation energy is dependent on the instantaneous structure of protonated Schiff base generated during the molecular dynamics simulation, which is further influenced by the dynamic fluctuations of the protein conformation. At any dynamics step, the PSB structure deviates from its optimal geometry in the gas phase. Consequently, the use of either the gas-phase geometry embedded in the protein environment or a structure minimized in the presence of a fixed protein configuration does not provide a full picture of the observed spectra. The spectral shifts can be obtained by ensemble averaging over the molecular dynamics trajectory.

We used 50 configurations that were saved during the last 500 ps of the molecular dynamics simulation at a 10-ps interval to analyze the spectral properties using QM-CIS/MM calculations. This was performed following the following procedure. For each configuration generated by the dynamics simulations using the classical force field, we further carried out combined QM/MM simulations, in which the PSB chromophore was treated by the semiempirical AM1 method.[93] In these simulations, we propagated 200 steps of molecular dynamics integration starting with the initial velocities and forces from the classical simulation. The primary purpose of these short QM/MM simulations is to obtain a more reliable instantaneous molecular geometry for the PSB than that generated using the force field. The semiempirical AM1 model can yield good results in molecular geometry for hydrocarbon compounds[93] such as the retinal polyene system. The resulting structures are then used in the electronic spectral calculation employing an ab initio QM/MM potential.

The structures for the mutant rhodopsins were generated by replacing the side chain atoms of the corresponding amino acid in the wild-type protein by the mutant residue with the maximum overlap for those atoms present in both residues. The side chain of the mutated residue is then subjected to 50 steps of minimization to optimize the bond lengths and bond angles. This is followed by a short 100-step dynamics simulation for the neighboring residues within 5 Å radius of the mutated residue, primarily to relax the environment around the point of mutation. In this case, the chromophore coordinates were held fixed throughout the mutation protocol. The ensemble of structures thus generated was used for the calculation of electronic excitation energies and the study of mutation effects on the absorption characteristics of the chromophore.

D. Absorption Energy Shift—We consider the thermodynamic cycle shown in Scheme 1, which relates the experimental opsin shift, $\Delta\nu(\mathrm{OS})$, to the changes in the excitation energy due to retinal conformational change $\Delta\nu(\mathrm{conf})$ in the gas phase, solvation $\Delta\nu(\mathrm{sol})$, and PSB-protein interactions $\Delta\nu(\mathrm{rhod})$. Thus,

$$\Delta\nu(OS)=\Delta\nu(conf)+\Delta\nu(rhod)-\Delta\nu(sol) \quad (1)$$

The first term in eq 1 relates to the intrinsic conformational change in the chromophore when transferred from solution (6-s-cis) to the protein (6-s-cis/11-s-cis) environment. To estimate the $\Delta\nu(\mathrm{conf})$ term, configuration interaction calculations with single excitations (CIS) using the 3-21/G and 6-31G(d) basis sets along with an active space of 60 occupied and 50 unoccupied orbitals were performed.[73] Although higher level of theory can be used here to obtain more accurate results in the absolute transition energy,[28–42] the present study focuses on the shift in the excitation energy and the CIS method can yield reasonable results.[22,68–70] Since the QM-CIS/MM approach is used in the solution and protein systems, we choose to use the same procedure for the gas-phase process. We also found that the results obtained using the two basis sets are very similar and we have decided to use the 3-21G basis set in all calculations on the protein and solution systems.

The second and third terms in eq 1 relate to effects of solvation on the protonated Schiff base by the protein-aqueous environment and in methanol solution. This requires the construction of an integrated protein-lipid bilayer system and averaging the computed spectral shifts over a molecular dynamics trajectory that includes configuration sampling. The effects of methanol solvation on PSB have been investigated previously in combined QM-CIS/MM simulations.[22]

The excitation energies of the PSB for the ensembles of structures were obtained using the program GAMESS,[94] which has been modified to include the effect of the electric fields of the protein-lipid and solvent environment.[22,95,96] The chromophore was described using ab initio molecular orbital theory at the CIS/3-21G level with an active space of 60 occupied orbitals and 50 lowest virtual orbitals. As noted above, although the CIS method is poor at predicting the vertical absolute excitation energies, it has been found to perform adequately to account for environment-induced shifts.[22] In the present calculation, the spectral shifts are determined by subtracting excitation energy of the reference molecule in the gas phase from the computed vertical excitation energy in rhodopsin.[22]

The retinal chromophore along with part of the covalently linked Lys296 is treated by the semiempirical AM1 model, and the generalized hybrid orbital (GHO)[97] method was employed to describe the boundary between the quantum and classical regions, which is located at the C_δ atom of Lys296. CIS calculations with the inclusion of the solvent environment as point charges were then performed on an ensemble of AM1/CHARMM-TIP3P-equilibrated structures.[22,43,68–70,98] Inclusion of the effects of the instantaneous polarization of the environment by using a polarizable force field tends to stabilize the excited state for electronic transitions that lead to charge delocalization, but this effect is typically small for systems that have been examined with contributions about 10 to 100 cm^{-1}.[69,70,98,99] For rhodopsins, Wanko et al. found that the instantaneous polarization of the protein environment in response to the electronic excitation of the PSB reduces the vertical excitation energy by about 30 cm^{-1} (0.05 eV).[26,27]

The third term in eq 1 require statistical sampling of the retinal PSB in solution, for which we performed QM-CIS/MM Monte Carlo simulations of the 6-s-cis methylretinyledene protonated Schiff base without and with a chloride counterion at distances from 4 to 10 Å in a box (ca. 26.5 × 26.5 × 40 $Å^3$) of 385 methanol molecules modeled by the OPLS potential.[100]

Results and Discussion

We first present the results on the opsin shift of bovine rhodopsin. Then, we focus on the effects of individual amino acid mutations on the absorption energy of the chromophore.

A. The Opsin Shift—A three-step computational approach was utilized to estimate the opsin shift of the PSB in going from methanol to the rhodopsin-membrane environment (Scheme 1).[22] The first step involves the calculation of the change of absorption energy due to solvent effects by transferring 6-s-cis methylretinyledene protonated Schiff base from the gas phase into a methanol solution.[101–103] The second step yields the difference in exicitation energy arising from conformational change from the 6-s-cis/all-*trans* former preferred in solution to the 6-s-cis/11-*cis* structure corresponding to that in rhodopsin. The final step accounts for the effects of the rhodopsin-membrane-water environment on absorption energy of the 11-*cis* PSB.

The solvatochromic shift arising from the transfer of 6-s-cis methylretinylidene from the gas phase into methanol solution was computed by combined QM-CIS/MM Monte Carlo simulations.[22] The calculation included PSB chromophore along with a Cl^- counter ion in a box (~ 26.5 × 26.5 × 40 $Å^3$) of 385 methanol molecules. The PSB was described by the semempirical AM1 method[93] while the solvent was treated using Jorgensen's OPLS potential for methanol.[89,100] CIS excitation energies were averaged over 5000 configurations following every 50,000 Monte Carlo moves for a total of 2×10^6 configurations. The calculations were also performed without the chloride counterion, which did not change the quantitative results significantly, which is consistent with experiments showing little counterion effects on the UV-vis absorption spectra. To verify the

semiempirical results, CIS calculations on 20 structures saved during the simulation were repeated using the CIS/HF/3-21G method with an active space of 60 occupied and 50 unoccupied orbitals. A solvatochromic blue shift of 3250 ± 70 cm^{-1} at the semiempirical level and 3100 ± 50 cm^{-1} at the ab initio level were obtained in methanol solution with a chloride counterion. For comparison, the computed spectral shifts are 3030 ± 70 and 2900 ± 50 cm^{-1}, respectively, without the counter ion. Interestingly, although solvent effects are similar in acetonitrile solution, the presence of a counter ion in the aprotic solvent has greater impact on the absorption energy (Table 1). Surprisingly, there is smaller solvatochromic shifts in aqueous solution, which we attribute to hydrophobic effects. Concomitantly, counter ion contribution further diminishes in water due to favorable solvation of the small ion.

The energy difference arising from the 6-s-cis/all-trans to the 6-s-cis/11-cis conformation of the PSB in the gas phase was obtained by CIS/6-31G(d) and CIS/3-21G calculations with an active space of 60 occupied and 50 unoccupied oribitals. A red shift of about −204 cm^{-1} was obtained for the Δν(conf) term.

To evaluate the effects from the dynamical fluctuations of the protein environment embedded in the lipid membrane, we have carried out molecular dynamics simulations of protein-lipid-water system employing a molecular mechanics force field.[84–89] The average shift in absorption energy was determined by ab initio CIS-QM/MM single-point energy calculations based on structures that were saved along the dynamics trajectory. For each configuration, we first perform a short dynamics simulation using the combined AM1/CHARMM potential to further equilibrate the chromophore structure. The protein environment stabilizes the ground state of the PSB, resulting in an average blue shift of 2120 cm^{-1} relative to the gas phase value for the 6-s-cis/11-cis conformation. Combining the above three contributions, a net red shift of −’1180 (≈ − 3100 − 204 + 2120) cm^{-1} was estimated without the inclusion of dispersion contributions, which is may be compared with experiment (−2730 cm^{-1}).[61,101,102]

Our model is essentially a point charge model, in which the dispersion contribution due to interactions between the ground and excited states of the PSB with the MM environment is excluded.[68] However, this is different than the original point-charge model proposed by Honig and Nakanish and coworkers,[17,18,46–48] in that a specific counterion or counerions are involved. The present results represent the overall effects of electrostatic interactions in solution and in rhodopsin. A complete treatment of the problem must include dispersion effects, which would require the computation of the correlation energies between singly excited states for both the chromophore and all solvent molecules[104,105] and are computationally intractable.[68] Birge and co-workers, in their study of the spectral tuning in sensory Rhodopsin II, estimated the dispersion effects arising from the environment by including residues within 5 Å of the chromophore (charged residues within 12 Å).[20,21] Other approaches for the inclusion of dispersion effects have been reported in the literature.[104,105] Houjou et al.,[19,106] in their study to delineate the origin of the opsin shift in bR, employed a linear regression analysis of the experimental and theoretical solvatochromic shifts to derive a linear relationship that correlates the spectral shifts to the solvent's dielectric constant and refractive index. Based on the estimate of the refractive index for the PSB binding pocket in bR, a red-shift of 1000 cm^{-1} was estimated.[19] Adopting the estimate for dispersion contributions by Houjou et al,[19] we obtain at a best estimate of the opsin shift at about −’2100 cm^{-1} (red-shift) for rhodopsin, in reasonable agreement with experiments (−’2730 cm^{-1}).[61,101]

The present study and our previous study on the opsin shift of bR have shown that the solvent and protein environment provide greater stabilization for the ground state than the π*

excited state (greater charge delocalization). Both specific hydrogen bonding and non-specific electrostatic interactions contribute to the solvatochromic blue shift of the PSB in methanol solution. The relative effect due to the electrostatic interactions in the protein-membrane environment is smaller that that in methanol by 980 cm^{-1}. The contributions arising from the change in retinal conformation is relatively small (ca. 200 cm^{-1}), while dispersion interactions make large contributions due to the presence of aromatic residues along the polyene chain.[19]

To provide further insights into the effect of dynamic structural fluctuations of the PSB on the computed spectral shifts, we have also computed the absorption energy of the PSB in the gas phase, but using ten instantaneous structures of the PSB in the rhodopsin-membrane-water configurations from the combined QM/MM simulations. This also yields the electrostatic effects of protein-membrane environment due to “vertical” solvation of the twisted, instantaneous chromophore. Table 2 lists the results of the energy decomposition analysis, which shows that the change of the chromophore structure due to dynamic fluctuations increases the energy gap between the ground state and the excited state, mainly due to the change of single-double bond distance alternation. The change in bond length alternation has been shown to have direct correlation with calculated vertical excitation energies in rhodopsin environment.[24,25] However, the structural changes due to dynamic fluctuations are broader and greater than that obtained from geometry optimizations on selected structures,[22,43] and this emphasis the importance of dynamics simulations to incorporate these instantaneous structural variations.

B. Ionone Ring Conformation—Due to its role in activation of the protein, the orientation of the β-ionone ring with respect to the rest of the chromophore has been the focus in a number of studies.[106–109] Studies including the use of structurally locked retinal derivatives,[110] solid state NMR,[108,111] and geometry optimization using density functional theory (DFT) demonstrate that the rhodopsin chromophore has a preferred 6-s-cis orientation in the dark-adapted protein.[109] Spooner et al.[111] estimated a torsional angle of −28° ± 7° for C5-C6-C7-C8 on the basis of solid state NMR data derived from ^{13}C labeled 11-Z-retinal substrate. Sugihara et al. used the self-consistent-charge density functional based tight-binding (SCC-DFTB) method to map the preferred conformation of the chromophore in the active site.[109] In this work, residues within 4.5 Å of the PSB (27 amino acids) were used to mimic the retinal-binding environment and geometry optimization and constrained molecular dynamics simulations resulted in a preferred conformation of 6-s-cis configuration with a dihedral twist of −35°.

Figure 2 shows the distribution of the instantaneous dihedral angle (C5-C6-C7-C8) for the 50 structures generated from MM and combined QM/MM simulations, in which the PSB and part of Lys296 were treated at the AM1 level. There are two sets of conformers, corresponding to dihedral angles of −68° ± 55° and +68° ± 25° for the 6-s-cis configuration. In the gas phase, the energies of the two conformers are identical; however, a large fraction (86%) of the structures have a negative dihedral indicating the enzyme environment induces a preference for one of the two 6-s-cis conformations at the β-ionone ring. A statistical weighted average of −49° is predicted for the C5-C6-C7-C8 dihedral angle, which is reasonably consistent with experiments.[111,112]

C. Mechanism of Spectral Tuning—The effects of mutation were modeled by replacing a set of four residues through atom replacement and constrained minimizations (50 steps) of the side-chain of the mutated residue. This is then followed by a short molecular dynamics run of 100 steps involving residues within a 5 Å radius of the mutated residue. The occurrence of the four residues in relation to the retinal protonated schiff base is shown in Figure 3, which includes two mutations that could potentially reduce or increase the

strength of hydrogen-bonding interactions at the PSB site, and two that alter electrostatic interactions with the polyene chain and the β-ionone ring. The first two mutations are expected to have greater effects on the electronic ground state since they are in the PSB binding site as a counterion or forming a hydrogen bond, whereas the other two mutations would have stronger impact on the excited state due to charge propagation up on photoexcitation. All 50 structures from the ensemble for the wild-type protein were used in the calculations of the mutants. Figure 4 shows the distribution of the computed spectral shifts relative to the excitation energy of the wild-type reference structure.

C.1. Glu113Asp: The residue Glu113 has been proposed to be the primary candidate as the counterion of the protonated Schiff base,[49–51] which has been confirmed by the X-ray structure.[52,75] Sakmar and coworkers carried out site-directed mutagenesis experiments at this position,[113] and found that the Glu113Asp (E113D) mutation resulted in a red shift of 10 nm (−390 cm^{-1} in energy) in the maximum absorption wavelength compared to the wild-type rhodopsin. In our computation, we obtained a computed red-shift of −580 ± 250 cm^{-1} (Figure 4), which is in good accord with experiment. The spectral shift is attributed to electronic ground state destabilization due to the E113D mutation. As a counterion, Glu113 is positioned through evolution to interact with the PSB cation. The mutation to an Asp residue moves the counterion further away from the PSB because of the shorter side-chain length. Consequently, this reduces its ability to stabilize the protonated Schiff base, but the effect is smaller in the excited state because the cationic charge is more delocalized than that in the ground state, resulting in a net ground-state destabilization effect. Although dynamics fluctuations of the protein and chromophore would undoubtedly reduce this effect, the E113D mutant is no longer interacting with the PSB in an ideal orientation.

C.2. Ala292Ser: In a study designed to understand the mechanism in the green-to-blue opsin shift, Lin et al. identified twelve residues that may have important contributions based on sequence comparison between the bovine rhodopsin and mammalian blue cone pigment.[61] They found that 80% of the observed opsin shift (or 2830 cm^{-1}) between bovine rhodopsin and the blue-cone pigment can be accounted for by simultaneously substituting nine of the twelve residues in bovine rhodopsin by those in the blue pigment.[61] It was found that the introduction of hydroxyl groups at positions Gly90 (400 cm^{-1}), Ala292 (490 cm^{-1}) and Ala295 (200 cm^{-1}) yields a total of about 1000 cm^{-1} of blue shift. Ala292 is particularly interesting because of its proximity to the Schiff base. In the present study, we found that the Ala292Ser (A292S) mutation yields a small blue shift of 70 ± 240 cm^{-1} (Figure 4), which is smaller than the experimental value of 490 cm^{-1}. Altun et al. also obtained small blue shifts in the A292S mutation by energy minimizations on selected sidechain conformations.[24] Two factors may contribute to the difference in quantitative agreement with experiment. First, the computed spectral shifts have large fluctuations, suggesting that more structures may be needed in the ensemble average. Second, the mutant system was equilibrated with the chromophore held rigid, which may have prevented the serine mutant to interact with the protonated Schiff base more favorably. The results may be improved by running explicit QM/MM simulations of the mutant protein that average over a broader range of configurations to computed the spectral shifts. Nevertheless, the present study does yield a small blue shift and shows that the serine mutant forms a weak hydrogen bond with the PSB, affecting the chromophore's absorption energy.[114–119] The possible involvement of hydrogen-bonding interactions between the A292S mutant and the PSB has been discounted based on Raman data.[61] However, the absorption spectral data are a more direct probe of the specific interactions between the chromophore and its surrounding neighbors. The A292S mutation has the opposite effects in comparison with that of E113D in that the ground state of the PSB is more stabilized than the excited state due to the introduction of a hydrogen bond, which increases the energy gap between the ground and the excited state.

C.3. Thr118Ala: The crystal structure of bovine rhodopsin shows that Thr118 is positioned near the center of the polyene chain of the retinal chromophore in the vicinity of the C9-methyl group.[52,72] In a study to engineer a maximally blue-shifted rhodopsin mutant, Janz and Farrens identified Thr118 as a residue that can be mutated to produce a "blue-mutant", [120] and, in fact, the Thr118Ala (T118A) mutation leads to16 nm blue-shift in the absorption maxima, corresponding to an increase in the energy gap between the ground and excited state by 660 cm^{-1}. Computationally, we obtained a blue-shift of 160 ± 150 cm^{-1} by mutating Thr118 into an Ala (Figure 4). Although the quantitative agreement with experiment is not perfect, the qualitative trend is consistent with experiment and the mechanism of the spectral shift due to the T118A mutation is interesting. The computed spectral shift can be rationalized by excited-state electrostatic destabilization. Following electronic excitation, the charge distribution of the PSB becomes more delocalized through charge migration along the polyene chain in the direction toward the β-ionone ring. Thr118 in the wild-type rhodopsin provides electrostatic stabilization of the charge delocalized configuration of the excited state by the hydroxyl group, whereas the T118A mutant has a diminished electrostatic contribution. Consequently, the excited state is not as strongly stabilized in the mutant as that in the wild-type protein, leading to an increase in the energy gap and a blue shift. The effect of the T118A mutation has been attributed to other factors, including structural perturbation of the transmembrane helix-3, which affects the position of the counterion Glu113 in addition to local structural changes.[120] Note that the effect of Glu113 is primarily in the stabilization of the protonated Schiff base, which is a ground state effect. Although this might be possible, the effect of diminished dipolar stabilization of the excited state due to the T118A mutation from the computational study is consistent with experiment.

C.4. Ala269Thr: Chan et al. addressed the mechanism of spectral tuning between green and red pigments by mutating three residues (Ala164Ser, Phe261Tyr, Ala269Thr) common to bovine rhodopsin and the green pigment into amino acids found at the corresponding positions of the red visual pigment.[60] Their selection of residues was based on an earlier proposal by Neitz et al.,[63] who identified these substitutions to be the origin of the roughly −1000 cm^{-1} difference in absorption energy at λ_{max} between the green and red visual pigments. The double mutant F261Y/A269T yielded a total spectral shift of −775 cm^{-1}, while the single mutant A269T produces a red-shift of −545 cm^{-1}. These results led Chan et al. to suggest that interactions involving hydroxyl bearing amino acids with the chromophore may be a common mechanism in the adjustment of absorption energies among visual pigments.[60] A269 is located 5 Å from the β-ionone ring and the A269T mutation provides an interesting case, in which mutations away from the protonated Schiff base site can also play a major role in the spectral tuning. Our computation yields an average value of −210 ± 140 cm^{-1} energy shift (Figure 4), which may be compared to the experimentally red-shift of −545 cm^{-1}.[60] The origin of the spectral shift in the A269T mutation is due excited state stabilization, opposite to the case of T118A mutation, which is more significant due to stronger electrostatic or dipolar interactions between the Thr hydroxyl group and the charge delocalized excited state that develops greater cationic charge character at the ionone ring than in the ground state. For comparison, Altun et al. also examined the A269T mutation in their energy minimization calculations and obtained an average red shift of -14 cm^{-1} over four conformers.[24] These authors attributed the spectral change to the ground-state effect of decreased bond length alternation. Notice that the results in Table 2 (third column) show that the spectral fluctuations (±1880 cm^{-1}) are more than two orders of magnitude greater than that from minimized structures, and the computed spectral shifts are entirely due to electrostatic effects from the protein environment since the chromophore geometries are the same in the wild-type rhodopsin and the four mutant systems. It would be of interest in future studies to examine the effects of structural fluctuations due to amino acid mutations in dynamics simulations.

Conclusions

Molecular dynamics simulations and combined QM/MM calculations have been used to investigate the mechanism of the opsin shift and spectral tuning in rhodopsin. The present study provided confirmation for the understanding of the factors that contribute to the observed opsin shifts of bovine rhodopsin relative to that of the protonated Schiff base in methanol solution. Significant modulation in the absorption characteristics of the chromophore due to both the solvent and protein environment is observed. A significant red shift of −980 cm^{-1} was estimated due to the transfer of the chromophore from the solution environment to the PSB binding site of the opsin. Conformational change from a 6-s-cis-all-trans configuration in solution to a 6-s-cis-11-cis conformer contributes additional −200 cm^{-1} and the remaining effects arise form dispersion interactions with the aromatic residues present in the active site. Based on the estimate of a red-shift of 1000 cm^{-1} due to dispersion by Houjou et al. along with our simulation results on conformational and electrostatic effects, we obtain an opsin (red) shift of 2100 cm^{-1}, in reasonable accord with the experimental value of 2730 cm^{-1}. Structurally, we found that an average dihedral angle of −50° for the 6-scis bond, which is a result of two major conformation populations that restrict the β-ionone ring orientation. This may be compared with the experimental value of −28° ± 7° from solid-state NMR and Raman data. We investigated a series of four single-mutations, including E113D, A292S, T118A and A269T, which are located near the protonated Schiff base, along the polyene chain of retinal and close to the ionone ring. The computational results on absorption energy shift provide insights into the mechanism that visual pigments use for spectral tuning, which involve all means of electronic structural effects, including the stabilization or destabilization of either the ground or the electronically excited state of the retinal protonated Schiff base. In the case of Glu113Asp, ground state destabilization is the main factor that reduces the energy gap between the ground and the excited state, leading to a computed red-shift of −580 ± 250 cm^{-1} (expt: −390 cm^{-1}). On the other hand, ground state stabilization plays a major role in the Ala292Ser mutation due to the introduction of a hydrogen bond with the PSB, for which we obtained a computed blue-shift of 70 ± 240 cm^{-1} (expt: 490 cm^{-1}). The Thr118Ala mutation destabilizes the excited state by weakening electrostatic interactions with the charge density developed along the polyene chain in the excited state, giving rise to an estimated red- shift of 160 ± 150 cm^{-1} (expt: 660 cm^{-1}). Finally, the increased electrostatic interaction between hydroxyl group of the Ala269Thr mutant and the ionone ring favors excited state charge propagation, lowering the ground and excited state energy gap and resulting in a computed red-shift of −210 ± 140 cm^{-1} (expt: −545 cm^{-1}).[121]

Acknowledgments

This work was partially supported by the NIH (GM46376). All computations were performed at the Minnesota Supercomputing Institute.

References

1. Nathans J. Sci Am. 1989; 260:42. [PubMed: 2643825]
2. Sakmar TP, Menon ST, Marin EP, Awad ES. Annu Rev Biophys Biomol Struct. 2002; 31:443. [PubMed: 11988478]
3. Oprian DD, Asenjo AB, Lee N, Pelletier SL. Biochemistry. 1991; 30:11367. [PubMed: 1742276]
4. Merbs SL, Nathans J. Nature. 1992; 356:433. [PubMed: 1557124]
5. Mathies R, Oseroff AR, Stryer L. Proc Natl Acad Sci U S A. 1976; 73:1. [PubMed: 1061102]
6. Baldwin JM, Schertler GF, Unger VM. J Mol Biol. 1997; 272:144. [PubMed: 9299344]
7. Nakanishi K, Balogh-Nair V, Arnaboldi M, Tsujimoto K, Honig B. J Am Chem Soc. 1980; 102:7945.

8. Lythgoe, JN. Handbook of Sensory Physiology. Dartnall, HJ., editor. 1972. p. 604
9. Baltz PE, Mohler JH, Navanglu HV. Biochemistry. 1972; 11:848. [PubMed: 5059891]
10. Baltz PE, Mohler JH. Biochemistry. 1972; 11:3240. [PubMed: 5048286]
11. Arnaboldi M, Motto MG, Tsujimoto K, Balog-Nair V, Nakanishi K. J Am Chem Soc. 1979; 101:7082.
12. Bassov T, Sheves M. J Am Chem Soc. 1985; 107:7524.
13. Harbison GS, Smith SO, Pardoen JA, Courtin JML, Lugtenburg J, Herzfeld J, Matheis RA, Griffin RG. Biochemistry. 1985; 24:6955. [PubMed: 4074732]
14. Harbison GS, Mulder PPJ, Pardoen H, Lugtenburg J, Herzfeld J, Griffin RG. J Am Chem Soc. 1985; 107:4809.
15. Wada M, Sakurai M, Inoue Y, Tamura Y, Watanabe Y. J Am Chem Soc. 1994; 116:1537.
16. Van der Steen R, Biesheuvel PL, Mathies MA, Lugtenburg J. J Am Chem Soc. 1986; 108:6410.
17. Honig B, Dinur U, Nakanishi K, Balog-Nair V, Gwainowics MA, Arnaboldi M, Motto MG. J Am Chem Soc. 1979; 101:7084.
18. Hiroko K, Kakitani T, Rodman H, Honig B. Photochem Photobiol. 1985; 41:471. [PubMed: 4011704]
19. Houjou H, Inoue Y, Sakurai M. J Am Chem Soc. 1998; 120:4459.
20. Ren L, Martin CH, Wise KJ, Gillespie NB, Luecke H, Lanyi JK, Spudich JL, Birge RR. Biochemistry. 2001; 40:13906. [PubMed: 11705380]
21. Kusnetzow A, Dukkipati A, Babu KR, Singh D, Vought BW, Knox BE, Birge RR. Biochemistry. 2001; 40:7832. [PubMed: 11425310]
22. Rajamani R, Gao J. J Comp Chem. 2002; 23:96. [PubMed: 11913393]
23. Vreven T, Morokuma K. Theor Chem Acc. 2003; 109:125.
24. Altun A, Yokoyama S, Morokuma K. J Phys Chem B. 2008; 112:6814. [PubMed: 18473437]
25. Hoffmann M, Wanko M, Strodel P, König PH, Frauenheim T, Schulten K, Thiel W, Tajkhorshid E, Elstner M. J Am Chem Soc. 2006; 128:10808. [PubMed: 16910676]
26. Wanko M, Hoffmann M, Frauenheim T, Elstner M. J Phys Chem B. 2008; 112:11462. [PubMed: 18698712]
27. Wanko M, Hoffmann M, Frahmcke J, Frauenheim T, Elstner M. J Phys Chem B. 2008; 112:11468. [PubMed: 18729405]
28. Gascon JA, Batista VS. Biophys J. 2004; 87:2931. [PubMed: 15339806]
29. Gascon JA, Sproviero EM, Batista VS. Acc Chem Res. 2006; 39:184. [PubMed: 16548507]
30. Hufen J, Sugihara M, Buss V. J Phys Chem B. 2004; 108:20419.
31. Sekharan S, Weingart O, Buss V. Biophys J. 2006; 91:L07. [PubMed: 16648170]
32. Sekharan S, Sugihara M, Buss V. Angew Chem, Int Ed. 2007; 46:269.
33. Ferre N, Cembran A, Garavelli M, Olivucci M. Theor Chem Acc. 2004; 112:335.
34. Andruniow T, Ferre N, Olivucci M. Proc Natl Acad Sci. 2004; 101:17908. [PubMed: 15604139]
35. Cembran A, Gonzalez-Luque R, Altoe P, Merchan M, Bernardi F, Olivucci M, Garavelli M. J Phys Chem A. 2005; 109:6597. [PubMed: 16834008]
36. Coto PB, Strambi A, Ferre N, Olivucci M. Proc Natl Acad Sci. 2006; 103:17154. [PubMed: 17090682]
37. Blomgren F, Larsson S. J Comput Chem. 2005; 26:738. [PubMed: 15786429]
38. Tachikawa H, Kawabata H. J Photochem Photobiol B: Biol. 2005; 79:191.
39. Kazutomo K, Yamato T. Chem Phys Lett. 2006; 430:386.
40. Fujimoto K, Hasegawa J-Y, Hayashi S, Kato S, Nakatsuji H. Chem Phys Lett. 2005; 414:239.
41. Fujimoto K, Hasegawa J-Y, Hayashi S, Kato S, Nakatsuji H. Chem Phys Lett. 2005; 414:239.
42. Bravaya K, Bochenkova A, Granowsky A, Nemukhin A. J Am Chem Soc. 2007; 129:13035. [PubMed: 17924622]
43. Trabanino RJ, Vaidehi N, Goddard WA III. J Phys Chem B. 2006; 110:17230. [PubMed: 16928022]
44. Irving CS, Byers GW, Leermakers PA. Biochemistry. 1970; 9:858. [PubMed: 5417400]

45. Beppu Y, Kakitani T. Photochem Photobiol. 1994; 59:660.
46. Balogh-Nair V, Carriker JD, Honig B, Kamat V, Motto MG, Nakanishi K, Sen R, Sheves M, Tanis MA, Tsujimoto K. Photochem Photobiol. 1981; 33:483.
47. Nakanishi K, Balogh-Nair V, Gawinowicz MA, Arnaboldi M, Motto M, Honig B. Photochem Photobio. 1979; 29:657.
48. Honig, B. C. R. - Conf. Int. Spectrosc. Raman, 7th; 1980. p. 536
49. Sakmar TP, Franke RR, Khorana HG. Proc Natl Acad Sci. 1989; 86:8309. [PubMed: 2573063]
50. Zhukovsky EA, Oprian DD. Science. 1989; 246:928. [PubMed: 2573154]
51. Nathans J. Biochemistry. 1990; 29:9746. [PubMed: 1980212]
52. Palczewski K, Kumasaka T, Hori T, Behnke CA, Motoshima H, Fox BA, Trong I, Teller DC, Okada T, Stenkamp RE, Yamamoto M, Miyano M. Science. 2000; 289:739. [PubMed: 10926528]
53. Yan B, Spudich JL, Mazur P, Vunnam S, Dergini F, Nakinishi K. J Biol Chem. 1995; 270:29668. [PubMed: 8530353]
54. Froese RDJ, Komaromi I, Byun KS, Morokuma K. Chem Phys Lett. 1997; 272:335.
55. Blatz PE, Liebman PA. Exp Eye Res. 1973; 17:573. [PubMed: 4782841]
56. Honig B, Greenberg A, Dinur V, Ebrey T. Biochemistry. 1976; 15:4593. [PubMed: 974079]
57. Essen L-O. ChemBioChem. 2001; 2:513. [PubMed: 11828483]
58. Asenjo AB, Rim J, Oprian DD. Neuron. 1994; 12:1131. [PubMed: 8185948]
59. Nathans J, Thomas D, Hogness DS. Science. 1986; 232:193. [PubMed: 2937147]
60. Chan T, Lee M, Sakmar TP. J Biol Chem. 1992; 267:9478. [PubMed: 1577792]
61. Lin SW, Kochendoerfer GG, Carroll HS, Wang D, Mathies RA, Sakmar TP. J Biol Chem. 1998; 273:24583. [PubMed: 9733753]
62. Yokoyama R, Yokoyama S. Proc Natl Acad Sci. 1990; 87:9315. [PubMed: 2123554]
63. Neitz M, Neitz J, Jacobs GH. Science. 1991; 252:971. [PubMed: 1903559]
64. Kleinschmidt J, Harosi FI. Proc Natl Acad Sci U S A. 1992; 89:9181. [PubMed: 1409622]
65. Kochendoerfer GG, Wang Z, Oprian DD, Mathies RA. Biochemistry. 1997; 36:6577. [PubMed: 9184137]
66. Wang Z, Asenjo AB, Oprian DD, Mathies RA. Biochemistry. 1997; 32:2125. [PubMed: 8443153]
67. Nagata T, Oura T, Terakita A, Kandori H, Shichida Y. J Phys Chem A. 2002; 106:1969.
68. Gao J. J Am Chem Soc. 1994; 116:9324.
69. Gao J, Byun K. Theor Chem Acc. 1997; 96:151.
70. Lin Y-L, Gao J. J Chem Theory Comput. 2007; 3:1484.
71. Luzhkov V, Warshel A. J Am Chem Soc. 1991; 113:4491.
72. Hayashi S, Tajkhorshid E, Pebay-Peyroula E, Royant A, Landau EM, Navarro J, Schulten K. J Phys Chem B. 2001; 105:10124.
73. Foresman JB, Head-Gordon M, Pople JA, Frisch MJ. J Phys Chem. 1992; 96:135.
74. Karelson MM, Katritzky AR, Zerner MC. Int J Quantum Chem, Quantum Chem Symp. 1986; 20:521.
75. Teller DC, Okada T, Behnke CA, Palczewski K, Stenkamp RE. Biochemistry. 2001; 40:7761. [PubMed: 11425302]
76. Brooks B, Bruccoleri RE, Olafson BD, States DJ, Swaminathan S, Karplus M. J Comput Chem. 1983; 4:187.
77. Verhoeven MA, Creemers AFL, Bovee-Geurts PHM, DeGrip WJ, Lugtenburg J, De Groot HJM. Biochemistry. 2001; 40:3282. [PubMed: 11258947]
78. Eilers M, Reeves PJ, Ying W, Khorana HG, Smith SO. Proc Natl Acad Sci. 1999; 96:487. [PubMed: 9892660]
79. Nagata T, Terakita A, Kandori H, Kojima D, Schichida Y, Maeda A. Biochemistry. 1997; 36:6164. [PubMed: 9166788]
80. Zhang L, Hermans J. Proteins: Struct, Funct Genetcs. 1996; 24:433.
81. Woolf TB, Roux B. Proteins. 1996; 24:92. [PubMed: 8628736]
82. Nagle JF. Biophys J. 1993; 64:1476. [PubMed: 8324184]

83. Loof HD, Harvey SC, Segrest JP, Pastor RW. Biochemistry. 1991; 30:2099. [PubMed: 1998672]
84. MacKerell A, Bashford D, Bellot M, Dunbrack R, Evanseck JD, Feild M, Gao J, Guo H, Ha S, Joseph D, Kuchnir L, Kuczera K, Lau F, Mattos C, Minchnick S, Ngo T, Nguyen D, Prodhom B, Reiher WE, Roux B, Schlenkrich M, Smith J, Stote R, Strub J, Watanabe M, Wiokiewicz-Kuczera J, Yin D, Karplus M. J Phys Chem B. 1998; 102:3586.
85. Feller SE, Yin D, Pastor RW, MacKerell ADJ. Biophys J. 1997; 73:2269. [PubMed: 9370424]
86. Feller SE, MacKerell ADJ. J Phys Chem B. 2000; 104:7510.
87. Humphrey W, Logunov I, Schulten K, Sheves M. Biochemistry. 1994; 33:3668. [PubMed: 8142365]
88. Tajkhorshid E, Baudry J, Schulten K, Suhai S. Biophys J. 2000; 78:683. [PubMed: 10653781]
89. Jorgenson WL, Chandrasekhar J, Madura JD, Impey RW, Klein ML. J Chem Phys. 1983; 79:926.
90. Verlet L. Phys Rev. 1969; 159:98.
91. Rychaert J-P, Ciccotti G, Berendsen HJC. J Comput Phys. 1977; 23:327.
92. Darden T, York D, Pedersen L. J Chem Phys. 1993; 98:10089.
93. Dewar MJS, Zoebisch EG, Healy EF, Stewart JJP. J Am Chem Soc. 1985; 107:3902.
94. Shmidt MW, Baldrige KK, Boatz JA, Elbert ST, Gordon MS, Jensen JH, Koseki S, Matsunaga N, Ngyen KA, Su S, Windus TL, Dupuis M, Montgomery JAJ. J Comp Chem. 1993; 14:1347.
95. Gao J, Freindorf M. J Phys Chem A. 1997; 101:2962.
96. Freindorf M, Gao J. J Comput Chem. 1996; 17:3182.
97. Gao J, Amara P, Alhambra C, Feild MJ. J Phys Chem A. 1998; 102:4714.
98. Thompson MA. J Phys Chem. 1996; 100:14492.
99. Gao J. J Comput Chem. 1997; 18:1062.
100. Jorgenson WL. J Phys Chem. 1986; 90:1276.
101. Beck M, Sakmar TP, Seibert F. Biochemistry. 1998; 37:7630. [PubMed: 9585578]
102. Yan ECY, Kazmi MA, De S, Chang BSW, Seibert C, Marin EP, Mathies RA, Sakmar TP. Biochemistry. 2002; 41:3620–3627. [PubMed: 11888278]
103. Nielsen IB, Petersen MA, Lammich L, Nielsen MB, Andersen LH. J Phys Chem A. 2006; 110:12592. [PubMed: 17107108]
104. Rosch N, Zerner MC. J Phys Chem. 1994; 98:5817.
105. Cantuo S, Coutinho K, Zerner MC. J Chem Phys. 2000; 112:7293.
106. Houjou H, Inoue Y, Sakurai M. J Phys Chem B. 2001; 105:867.
107. Han M, Smith SO. Biochemistry. 1995; 34:1425. [PubMed: 7827090]
108. Grobner G, Brunett IJ, Glaubitz C, Choi G, Mason AJ, Watts A. Nature. 2000; 405:810. [PubMed: 10866205]
109. Sugihara M, Buss V, Entel P, Elstner M, Frauenheim T. Biochemistry. 2002; 41:15259. [PubMed: 12484764]
110. Sugihara M, Hufen J, Buss V. Biochemistry. 2006; 45:801. [PubMed: 16411756]
111. Spooner PJR, Sharples JM, Verhoveven MA, Lugtenburg J, Glaubitz C, Watts A. Biochemistry. 2002; 41:7549. [PubMed: 12056885]
112. Imamoto Y, Sakai M, Kutta Y, Wada A, Ito M, Schichida Y. Biochemistry. 1996; 35:6257. [PubMed: 8639566]
113. Sakmar TP, Franke RR, Khorana HG. Proc Natl Acad Sci. 1991; 88:3079. [PubMed: 2014228]
114. Chang BSW, Crandall KA, Carulli JP, Hartl DL. Mol Phylogenet Evol. 1995; 4:31. [PubMed: 7620634]
115. Sun H, Macke JP, Nathans J. Proc Natl Acad Sci U S A. 1997; 94:8860. [PubMed: 9238068]
116. Hope AJ, Patridge LC, Dulai KS, Hunt DM. Proc R Soc Lond B. 1997; 264:155.
117. Rao VR, Cohen GB, Oprian DD. Nature. 1994; 367:639. [PubMed: 8107847]
118. Nakayama TA, Khorana HG. J Biol Chem. 1991; 266:4269. [PubMed: 1999419]
119. Fahmy K, Zvyaga TA, Sakmar TP, Siebert F. Biochemistry. 1996; 35:15065. [PubMed: 8942673]
120. Janz JM, Farrens DL. Biochemistry. 2001; 40:7219. [PubMed: 11401569]

121. Rajamani, Ramkumar. PhD thesis. The University of Minnesota; 2004.

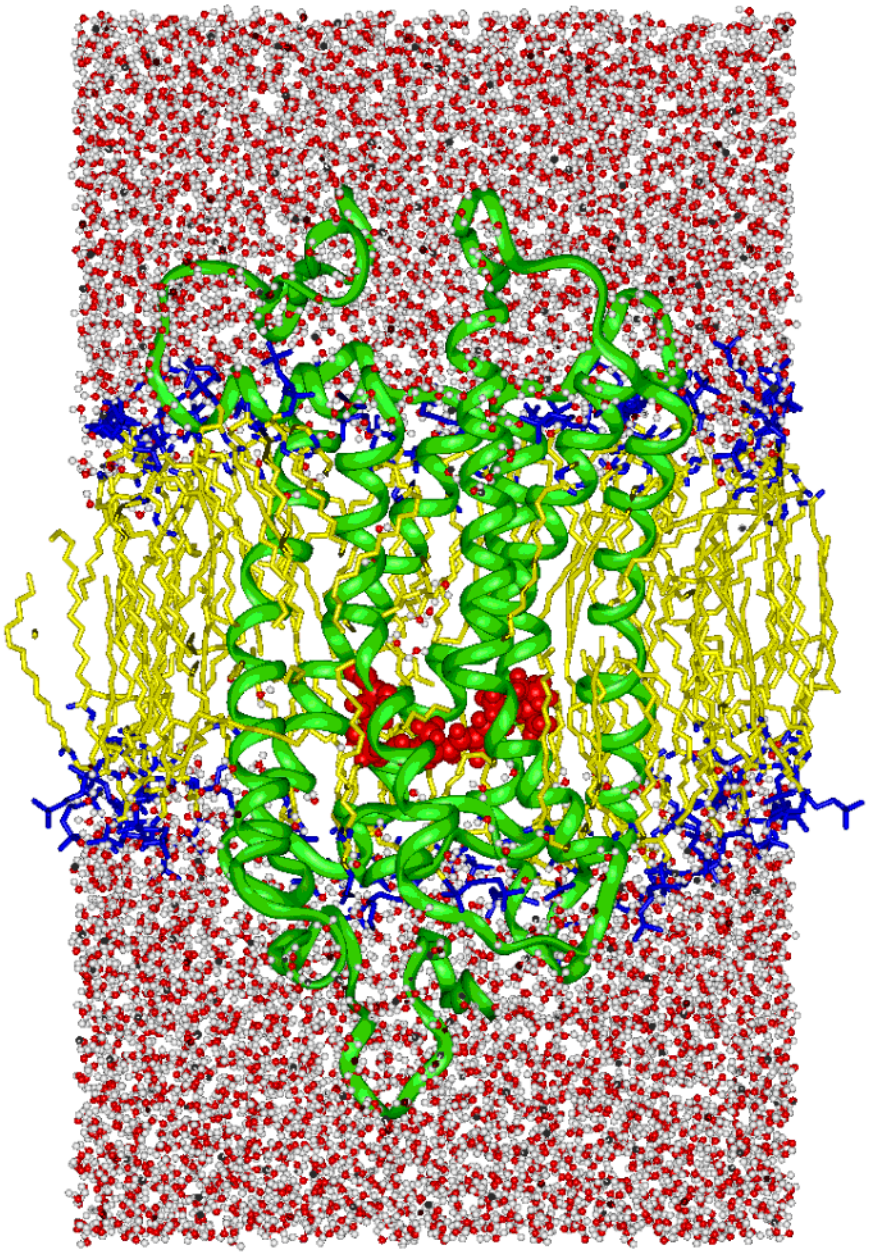

Figure 1.
A snapshot of the computational model. Rhodopsin is shown in green ribbon, retinal in red spheres, lipids in yellow and blue, and water in red and white spheres. Lipids and water molecules in front of the protein have been removed for clarity.

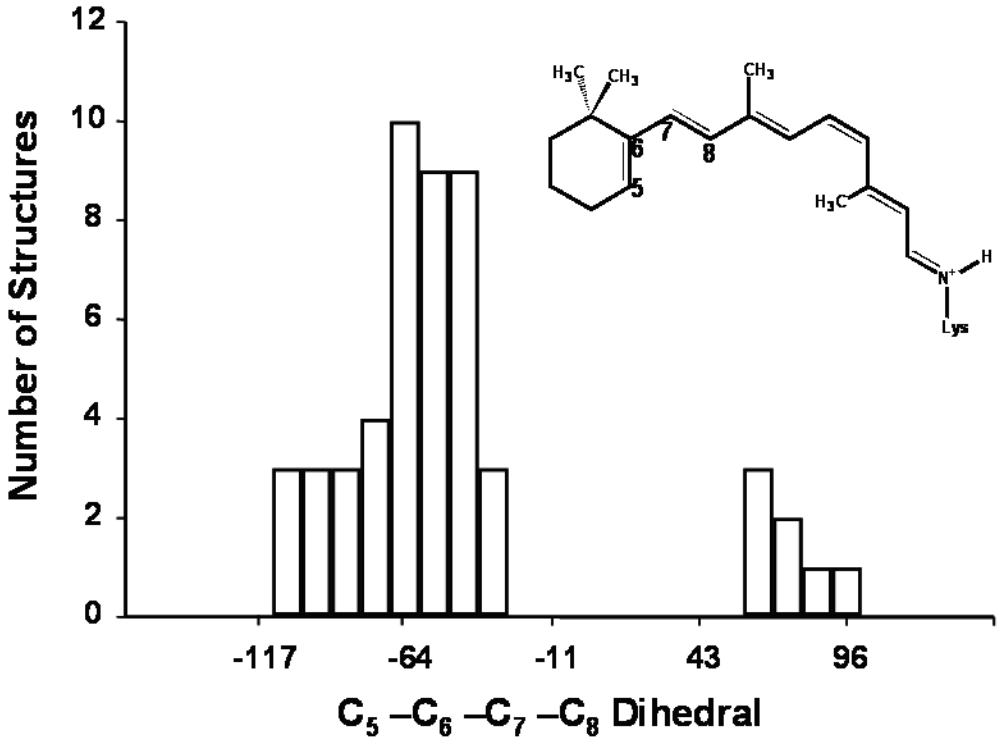

Figure 2.
Distribution of computed dihedral angles of the β-ionone ring of the retynylidene protonated Schiff base.

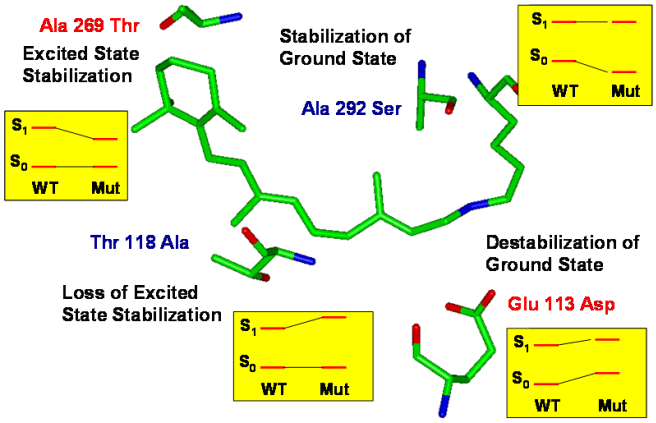

Figure 3.
Mechanism and schematic representation of the four selected residue mutations in the binding site of the retinal protonated Schiff base.

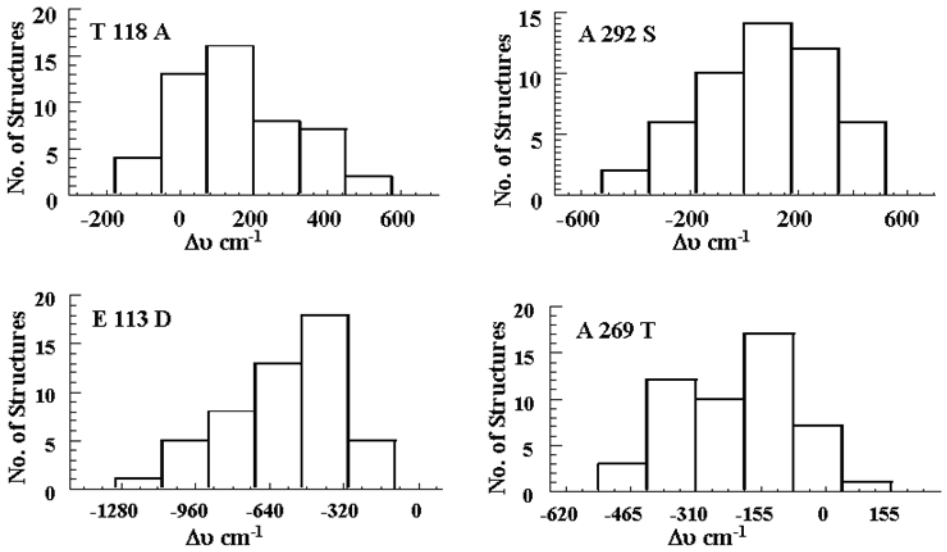

Figure 4.
Distribution of the computed spectral shifts in the excitation energy of the retinal chromophore due to residue mutations in rhodopsin.

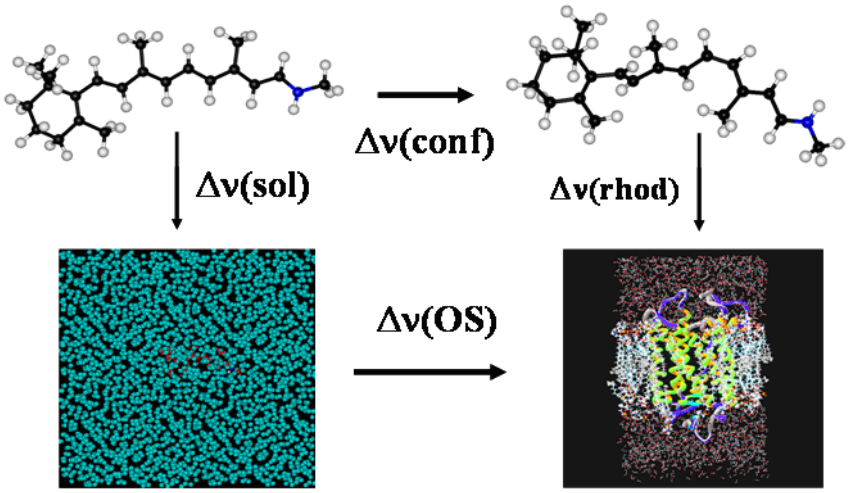

Scheme 1.
Thermodynamic cycle used for computing the rhodopsin shift.

Table 1

Computed average solvatochromic shifts of the protonated Schiff base 6-s-cis-methylretinylidene from the gas phase into solution (cm^{-1}).

	Without Cl^- counterion		With Cl^- counterion	
Solvent	**CIS/AM1**	**CIS/3-21G**	**CIS/AM1**	**CIS/3-21G**
CH_3OH	3030 ± 70	2900 ± 50	3250 ± 70	3100 ± 50
CH_3CN	3090 ± 70		3500 ± 80	
H_2O	2760 ± 90		2860 ± 70	

Table 2

Calculated absorption energies of the protonated Schiff base (PSB) in the rhodopsin-membrane system, and the corresponding PSB in the gas phase along with their difference. Energies are give in wave numbers (cm^{-1}).

Structure #	$PSB^{Protein}$	PSB^{Gas}	$(PSB^{Protein}- PSB^{Gas})$
1	32016	31359	657
2	30743	29980	763
3	31788	29738	2050
4	31239	29176	2063
5	30529	27247	3282
6	32042	30730	1312
7	30140	29430	710
8	35700	33797	1903
9	29779	27220	2559
10	29470	28198	1272
Average	31344 ± 1690	29687 ± 1883	1657 ± 824